

Thermal Lepton Production in Heavy-Ion Collisions

Ralf Rapp

Department of Physics and Astronomy,
SUNY Stony Brook, New York 11794-3800, U.S.A

Abstract. The current status of evaluating thermal production of lepton pairs in high-energy collisions of heavy nuclei is discussed. After a brief survey of emission rates from hot and dense matter, we address applications to (and interpretations of) recent SPS data including 40 AGeV CERES results, as well as prospects for NA60. Emphasis is put on predictions for RHIC. In particular, implications of hadronic observables and first single-electron measurements at $\sqrt{s} = 130$ AGeV for upcoming pair spectra from PHENIX at $\sqrt{s} = 200$ AGeV are assessed.

Keywords: Heavy-Ion Collisions, Dileptons, Chiral Symmetry Restoration
PACS: 25.75.-q, 12.38.Mh., 24.10.Pa

1. Introduction

Early on in the heavy-ion initiative, electromagnetic observables have been recognized as important probes of the hot and dense strongly interacting systems created in head-on collisions of nuclei at high energies [1, 2]. About 10-15 years later very exciting data on dilepton (and photon) spectra have emerged from the SPS heavy-ion program [3, 4, 5], stimulating vigorous theoretical activity (see ref. [6] for a recent review). All respective experiments have observed nontrivial excess production in heavy-ion collisions (increasing with centrality) over baseline expectations from p - p collisions (and/or final-state hadron decays), from threshold to about 3 GeV (dilepton invariant mass or photon transverse momentum). Indeed, these results imply strong evidence for some of the long sought-for signatures, such as in-medium modified vector mesons (especially the ρ) at low-mass ($M \leq 1$ GeV) or continuum-like thermal radiation from early phases at intermediate masses ($1 \text{ GeV} \leq M \leq 3 \text{ GeV}$). However, from the theoretical side, certain ambiguities in the detailed understanding and interpretation of the underlying dynamics remain at present.

The article is organized as follows: in Sect. 2 we briefly recall the theoretical framework suitable to evaluate equilibrium dilepton production rates and allude to specific model calculations. In Sect. 3 we turn to applications in heavy-ion collisions, starting with a discussion on chemical off-equilibrium effects in the hadronic phases in 3.1. In 3.2 we

highlight results for SPS energies including predicted spectra for $E_{lab} = 40$ AGeV as well as for a potential low-mass measurement by NA60. In 3.3 we present improved predictions for RHIC energies by incorporating information from measured hadron spectra. We also assess the role of thermal radiation in preliminary PHENIX single-electron spectra at $\sqrt{s}=130$ AGeV, and ensuing implications for upcoming pair spectra. In Sect. 4 we end with some concluding remarks.

2. Electromagnetic Correlation Function and Dilepton Radiation

2.1. E.M. Correlator in Vacuum

Dilepton emission from thermalized QCD matter can be characterized by the pair production rate per unit 4-volume and 4-momentum,

$$\frac{dR_{l+l-}^{therm}}{d^4q} = -\frac{\alpha^2}{\pi^3 M^2} f^B(q_0; T) \text{Im}\Pi_{em}(M, q; \mu_B; T) \quad (1)$$

($f^B(q_0; T) = 1/(\exp[q_0/T] - 1)$): Bose distribution function, $M^2 = q_0^2 - q^2 = (p_+ + p_-)^2$: invariant mass squared of the lepton pair with individual 4-momenta p_{\pm}). The key quantity encoding the information on the strongly interacting medium is the imaginary part of the electromagnetic current-current correlation function (or simply photon selfenergy), $\text{Im}\Pi_{em}$. In vacuum, it is directly related to the famous cross section ratio $R = \sigma_{ee \rightarrow hadrons} / \sigma_{ee \rightarrow \mu\mu}$ and can be decomposed into two invariant-mass regions:

$$\text{Im}\Pi_{em}(M) = \begin{cases} \sum_{V=\rho, \omega, \phi} \left(\frac{m_V^2}{g_V}\right)^2 \text{Im}D_V(M) & , M \leq M_{dual} \\ -\frac{M^2}{12\pi} \left(1 + \frac{\alpha_s(M^2)}{\pi} + \dots\right) N_c \sum_{q=u, d, s} (e_q)^2 & , M \geq M_{dual} . \end{cases} \quad (2)$$

At small distances, *i.e.*, $M \geq M_{dual} \simeq 1.5$ GeV, perturbation theory applies and the correlator strength follows from the (charge-square weighted) sum over free $q\bar{q}$ states (with rather small corrections); subsequent hadronization does not affect the strength. The experimental fact that hadron production in e^+e^- annihilation essentially follows thermal systematics allows the time-reversal of this argument: e^+e^- production from a thermal hadron gas is determined by the perturbative 'dual' strength given by Eq. (2). This has also been verified by explicit hadronic rate calculations [7].

At low M , the e.m. correlator is governed by nonperturbative dynamics encoded in resonance formation. The experimental distribution is well described by the light neutral vector mesons ρ , ω and ϕ (vector dominance model). Thus, in principle, dilepton spectra from heavy-ion reactions directly reflect upon medium modifications of vector mesons.

But one can go further and establish connections to chiral symmetry restoration. This necessitates the inclusion of the chiral partners of the vector mesons in the (theoretical) analysis. Within the standard (non-/linear σ -model type) interpretation, and for $N_f=2$ flavors, the $SU(2)$ chiral partner of the ρ is the $a_1(1260)$, whereas the ω is a singlet (for $SU(3)$

the octet- ω_8 and singlet- ω_0 mix into ω and ϕ rendering both non-invariant under chiral rotations). This is to be contrasted with the recently suggested 'Vector Manifestation' of chiral symmetry, where the longitudinal component of the ρ is identified as the chiral partner of the pion [8].

Spontaneous chiral symmetry breaking in the vacuum is nicely illustrated by hadronic τ decay data in terms of the difference between vector and axialvector spectral functions at low M^2 , cf. Fig. 1. It can be quantified via Weinberg sum rules, *e.g.*,

$$f_\pi^2 = - \int \frac{ds}{\pi s} (\text{Im}\Pi_V - \text{Im}\Pi_A) . \quad (3)$$

Above $M^2 \simeq 3 \text{ GeV}^2$, Π_V and Π_A degenerate signifying the onset of the perturbative regime.

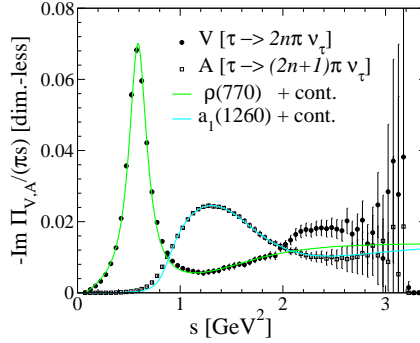


Fig. 1. Free isovector axial-/vector spectral functions from hadronic tau-decay data [9].

Finally note that the ρ -meson strength in the e.m. correlator dominates over the ω by about an order of magnitude (as reflected by the e.m. decay widths, $\Gamma_{\rho \rightarrow ee} = 6.8 \text{ keV}$ vs. $\Gamma_{\omega \rightarrow ee} = 0.6 \text{ keV}$, or the naive quark-model prediction $\Gamma_{\rho \rightarrow ee} / \Gamma_{\omega \rightarrow ee} = 9/1$).

2.2. Medium Effects and Dilepton Emissivities

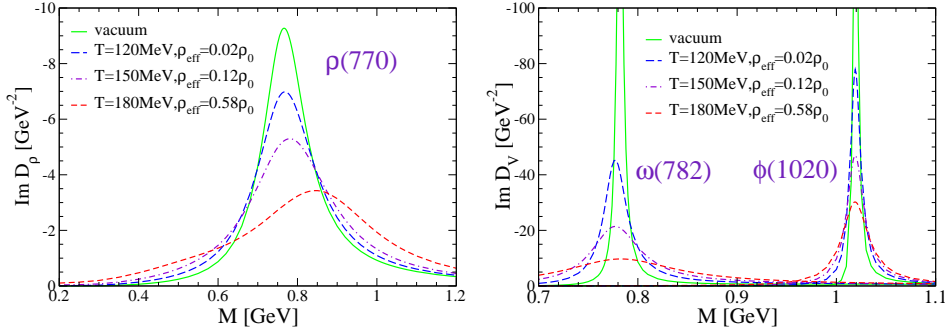
A compilation of the extensive investigations on in-medium modifications of the e.m. correlator (dilepton production rate) in both hadronic and quark-gluon phases is attempted in Table 1. As argued above, beyond masses of 1.5 GeV the rates are reasonably well understood with moderate α_s -corrections to $q\bar{q}$ annihilation in the QGP, and prevalent 4π -type annihilations (such as πa_1 or $\pi\omega$) in the hadron gas. The πa_1 channel, however, bears special relevance in the non-/perturbative 'transition region' between 1 and 1.5 GeV: it can be interpreted as a lowest order in temperature 'chiral' mixing (in parallel with $\pi\rho \rightarrow a_1$) [12] leading (for $M > 1 \text{ GeV}$) to a 3-fold degeneration of Π_V , Π_A and the pQCD continuum at temperatures not far from the expected T_c .

At low mass in the hadronic sector, substantial medium effects are predicted for ρ and ω mesons (less pronounced for ϕ mesons due to the OZI rule). Most approaches have reached consensus that baryon-induced effects dominate over meson-induced ones at comparable densities, even on a quantitative level [6, 14]. This seems to imply that

Table 1. Summary of medium effects in thermal dilepton production.

| | Hadron Gas | Quark-Gluon Plasma |
|--|--|--|
| Low Mass $M \lesssim 1$ GeV | in-medium ρ , ω , ϕ : effective chiral Lagrangian + VDM + finite- T / $-\mu_B$ field theory [6] $D_V = [M^2 - m_V^2 - \Sigma_V(M, q; \mu_B, T)]^{-1}$ | perturbative QCD: HTL-resummed $q\bar{q} \rightarrow ee$ [10] non-pert. QCD: gluon condensates ($T \gtrsim T_c$) [11] |
| Intermediate Mass $M \gtrsim 1$ GeV | $\pi a_1 \rightarrow l^+ l^-$ annihilation [7] $\hat{=}$ chiral V-A mixing [12] $\Pi_{V,A} = (1 - \epsilon) \Pi_{V,A}^0 + \epsilon \Pi_{A,V}^0$ | 'bare' α_s corrections to $q\bar{q}$ annihilation [13] order $O(\alpha_s \frac{T^2}{M^2})$ |

medium effects at heavy-ion colliders (RHIC and LHC), where the net baryon densities at midrapidity are small, are less pronounced. However, as pointed out in ref. [15], vector mesons equally interact with baryons and antibaryons, *i.e.*, the relevant quantity for medium effects is the *sum* of baryon and antibaryon density. Indeed, at midrapidities at RHIC [16], dN_B/dy is about as large as at SPS. An example of vector-meson spectral functions at small *net* baryon density is displayed in Fig. 2. At the highest temperatures ($T = 180$ MeV), $\sim 40\%$ of the medium effects stem from anti-/baryons.

**Fig. 2.** Light vector-meson spectral functions [15] in thermal and chemical equilibrium at fixed entropy-per-baryon characteristic for RHIC-200 conditions.

Pertinent 3-momentum integrated dilepton production rates are shown in Fig. 3 and compared to hadronic rates without medium effects (dotted curves), as well as to QGP emission to lowest order $O(\alpha_s^0)$ and within HTL-resummed perturbation theory [10]. One finds that even for small *net* baryon densities the in-medium hadronic and QGP results become remarkably similar when approaching the expected T_c , supporting the notion of quark-hadron duality towards low masses in the vicinity of the phase transition [17]. The key features are resonance melting in the hadronic, as well as soft emission characteristic for interacting many-body systems in both the hadronic and QGP phases.

3. Dileptons in Heavy-Ion Collisions

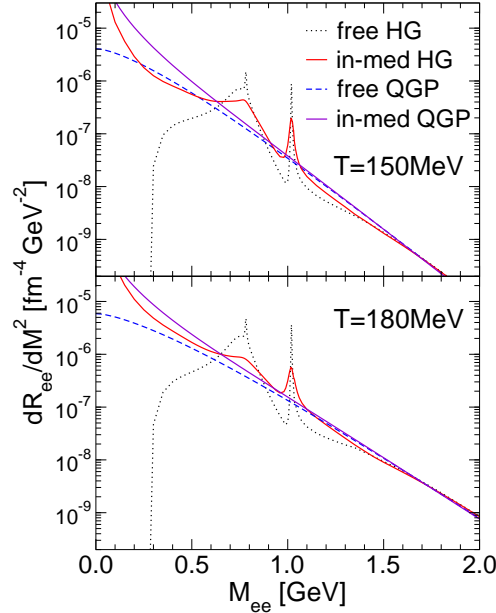


Fig. 3. 3-momentum integrated dilepton production rates from equilibrium matter with specific entropy characteristic for RHIC energies.

3.1. Thermal Production and Chemical Off-Equilibrium

Thermal dilepton production in heavy-ion collisions is calculated by a convolution of the rate given in Eq. (1) over the space-time history of the system. The natural dynamic framework are hydrodynamic [18, 19] (or simplified thermal fireball) simulations, being formulated in the same variables as the rates (temperature and baryon chemical potential). For invariant mass spectra, *e.g.*, one has (*Acc* indicates kinematic detector acceptance cuts)

$$\frac{dN_{l^+l^-}^{thermal}}{dM} = \int_{\tau_0}^{\tau_{fo}} d\tau V_{FB}(\tau) \int d^3q \frac{M}{q_0} \frac{dR_{l^+l^-}^{thermal}}{d^4q} Acc, \quad (4)$$

Clearly, a realistic space-time description must be consistent with hadronic observables.

With elastic hadronic cross sections being much larger than inelastic ones, thermal equilibrium in the expanding hadron gas phase is maintained longer than the chemical one. Therefore, subsequent to chemical freezeout (which for SPS energies and beyond essentially coincides with the expected phase boundary to the QGP) the effective numbers of non-strongly decaying particles have to be conserved. This can be implemented into the equation of state via additional (effective) chemical potentials for, *e.g.*, pions, kaons, etas and even antibaryons. These can have substantial impact on the composition and evolution of the hadronic system. In particular, the build-up of large pion-chemical potentials enhances thermal dilepton production through $\pi\pi$ annihilation [17], which is often neglected

in hydrodynamic calculations.

At RHIC energies, antibaryon-number conservation has appreciable consequences for low-mass dilepton spectra. If no corresponding effective chemical μ_B^{eff} is introduced, the anti-/baryon abundance at the later hadronic stages (assuming isentropic expansion) will be much reduced; at the same time, meson-chemical potentials seem to remain small [15]. On the other hand, imposing the individual anti-/baryon numbers to be constant throughout the evolution, and starting from full chemical equilibrium at $(\mu_N, T) = (25, 180)$ MeV, leads to anti-/baryon chemical potentials of up to $\mu_N \simeq 270$ MeV and $\mu_{\bar{N}} = -\mu_N + \mu_B^{eff} \simeq 230$ MeV at a temperature $T \simeq 130$ MeV. Due to entropy conservation one then also finds appreciable pion- and kaon-chemical potentials, *e.g.*, $\mu_\pi(T = 130 \text{ MeV}) \simeq 70$ MeV. To illustrate the impact on dilepton production, the vector-meson spectral functions along such a trajectory are displayed in Fig. 4. As compared to Fig. 2, one finds that chemical off-equilibrium reinforces medium effects at the later stages.

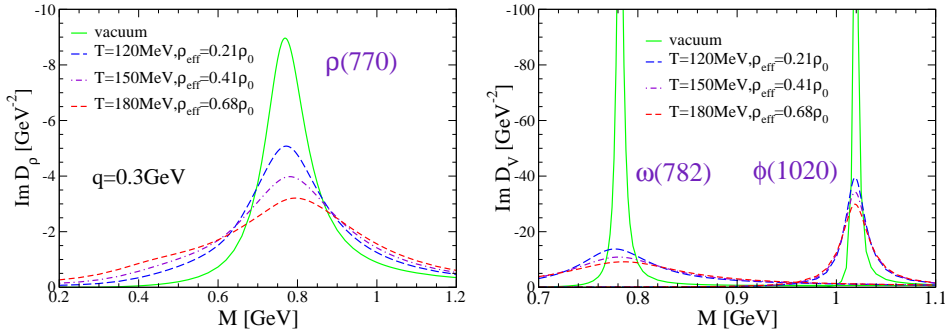


Fig. 4. Light vector-meson spectral function for RHIC-200 conditions including chemical-off-equilibrium effects.

An accurate identification of the thermal dilepton component furthermore hinges on a reliable knowledge of 'background' sources, such as e.m. hadron decays after freezeout (low mass), or Drell-Yan annihilation and correlated open charm decays (higher masses).

3.2. Post- and Predictions at SPS Energies

Numerous theoretical works have addressed the low-mass excess observed by the NA45 collaboration (CERES). The minimal conclusion at this point is that strong in-medium effects on the ρ -meson are needed to fill in the mass region around 0.4 GeV without overpredicting the yield around the free ρ - ω mass (which is largely saturated by the hadronic decay 'cocktail'). However, within the present experimental accuracy, it is not possible to discriminate the conjecture of a dropping ρ -mass from a ρ -melting (due to strong reinteractions in a hot and dense medium), as illustrated by thermal fireball calculations in Fig. 5.

The suggestion of the 'Vector Manifestation' of chiral symmetry [8] has, in fact, revoked interest in the 'dropping mass' scenario [21]. On the other hand, a recent finite-temperature analysis to one-loop order within a chirally symmetric hadronic model with realistic vacuum properties including a_1 -mesons lends further support to broadening as

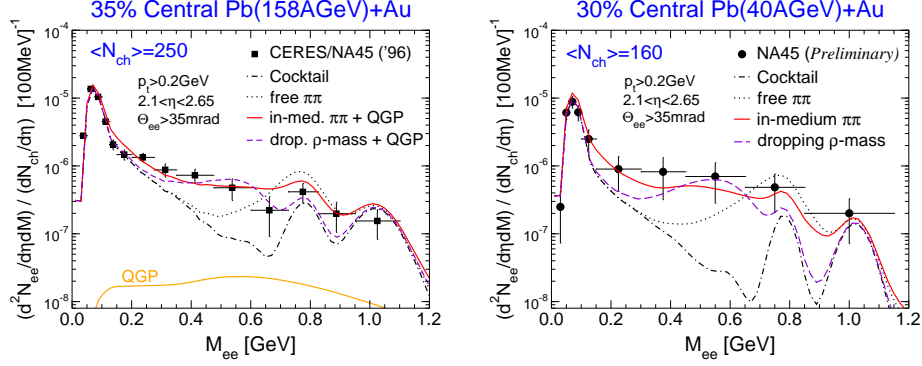


Fig. 5. Thermal fireball calculations [20] plus hadronic decay cocktail (dashed-dotted lines) compared to CERES data at full [3] (left panel) and lower [5] (right panel) SPS energies.

the prevalent in-medium modification of ρ and a_1 -mesons [22]. The essential difference between these approaches lies in whether medium effects in the bare parameters of the underlying interaction lagrangians are to be incorporated or not. The ensuing realizations of chiral symmetry restoration are obviously rather different. Nevertheless, within both scenarios stronger medium effects were predicted at lower SPS energies as being of baryonic origin, which is supported by available 40 AGeV CERES data (right panel in Fig. 5).

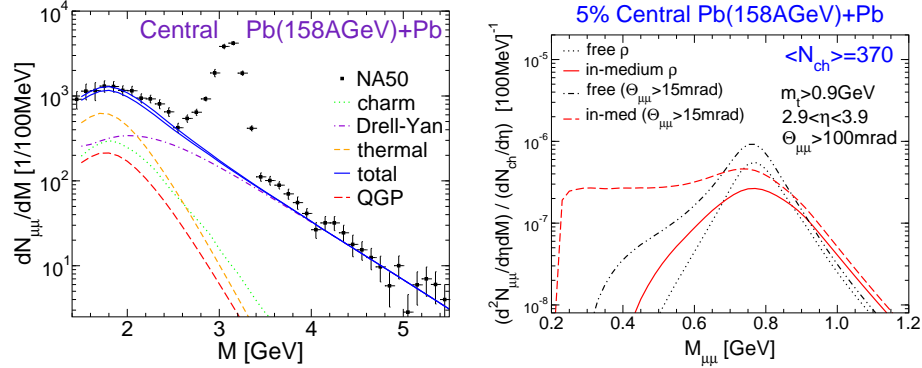


Fig. 6. Left panel: NA50 dimuon spectra [4] compared to a sum of pp -extrapolated Drell-Yan and open-charm sources plus thermal radiation [23]. Right panel: Low-mass prediction for an approximate NA60 acceptance.

Within the same thermal evolution framework, the intermediate-mass enhancement observed by NA50 can also be explained, cf. left panel of Fig. 6. At these higher masses, where the production rates are fairly well-established, one becomes more sensitive to the early stages of the collision, pointing at initial temperatures of ~ 220 MeV or so, well inside the QGP phase. For the future NA60 run it may also be interesting to provide a low mass prediction; this is shown in the right panel of Fig. 6 for the thermal contribution. One

realizes that with a sufficiently small opening angle cut, a substantial low-mass enhancement could be observed. But even with a large opening-angle cut, the peak-reduction of the in-medium prediction by a factor of 2 as compared to the vacuum spectral function persists. The situation is very similar at 40 AGeV (not shown).

3.3. Improved Predictions for RHIC

Before RHIC started operation, the common belief was that an enhanced particle production entails significantly longer fireball lifetimes than at SPS. Hadronic observables at RHIC show that dN_{ch}/dy at $\sqrt{s} = 200$ AGeV is indeed by a factor of 2 larger than at SPS ($\sqrt{s} = 17$ AGeV), but, surprisingly, the HBT source radii do not change much [24]. Although hydrodynamic simulations are currently not able to explain this feature, it can be easily incorporated in a suitable fireball parameterization of the expansion. We have employed such a phenomenologically improved description to assess the effect on dilepton spectra. In addition we have also incorporated antibaryon number conservation until thermal freezeout as delineated in Sect. 3.1. The resulting low-mass spectra are compared to the earlier prediction of ref. [15] in Fig. 7. As to be expected, the reduced fireball lifetime decreases the hadron gas yield somewhat [15], but, more importantly, the improved hadro-chemistry reinforces baryonic effects in terms of resonance broadening and low-mass enhancement.

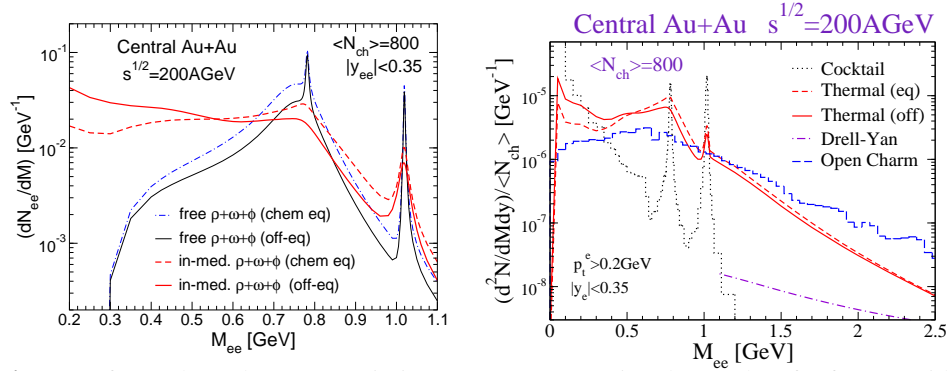


Fig. 7. Left panel: Hadron Gas emission at RHIC comparing the results of ref. [15] with those using an improved fireball evolution including chemical off-equilibrium and reduced lifetime; right panel: corresponding thermal spectra compared to hadronic cocktail and open-charm decays [25] as well as Drell-Yan annihilation.

The most severe physics background for dilepton spectra at collider energies are open-charm decays [26]; while those are subleading at SPS energies they may become dominant at RHIC, at least at intermediate masses, cf. right panel of Fig. 7.

The charm production cross section at RHIC energies is rather uncertain; first indirect evidence that it complies well with pp -based extrapolations from lower energies is provided by single-electron spectra measured by PHENIX at $\sqrt{s} = 130$ AGeV: charm decays nicely account for the excess over observed sources at $p_t^e \geq 1.5$ GeV. At the same time, the thermal

contribution to the single- e^\pm spectra turns out to be negligible. This situation changes in the pair spectra: the open-charm contribution is relatively suppressed to thermal radiation (especially at lower masses) by an additional semileptonic branching ratio, their harder spectral shape and the typically large rapidity gaps between e^+ and e^- (within the rather narrow PHENIX acceptance).

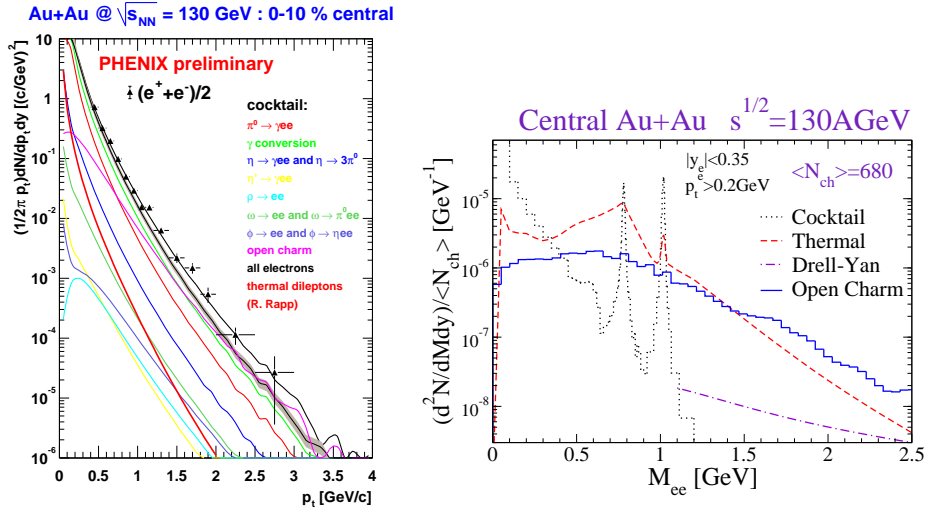


Fig. 8. Left panel: preliminary single-electron p_t spectra from PHENIX [27] compared to expected sources, as well as additional thermal and open-charm contributions. Right panel: corresponding e^+e^- pair spectra based on the same ingredients as the singles.

4. Conclusions

Dileptons continue to be an exciting probe in heavy-ion physics. From the theoretical side, more analysis is required to strengthen connections to chiral symmetry restoration, capitalizing further on recent progress. In particular, baryonic effects appear to play a key role. From a practical point of view it is thus encouraging to note that the (anti-) baryon driven impact on low-mass spectra remains appreciable at collider energies (reinforced by chemical off-equilibrium effects). In addition, the open-charm 'problem' seems sufficiently controllable (at least at RHIC) to enable the identification of thermal radiation (possibly even at intermediate masses, where it is of QGP origin). This raises the hope that the new generation experiments at GSI, CERN and RHIC will substantially advance our understanding of nonperturbative dynamics in the transition regions across the QCD phase diagram.

Acknowledgement

I thank the organizers for the invitation to this pleasant and stimulating workshop. This work is supported by the U.S. Department of Energy under grant no. DE-FG0288ER40388.

References

1. E.V. Shuryak, Phys. Rep. **61** (1980) 71.
2. L. McLerran and T. Toimela, Phys. Rev. **D31** (1985) 545.
3. CERES/NA45 Collaboration (G. Agakishiev *et al.*), Phys. Lett. **B422** (1998) 405.
4. NA50 Collaboration (M.C. Abreu *et al.*), Eur. Phys. J. **C14** (2000) 443.
5. CERES/NA45 Collaboration (D. Adamova *et al.*), Nucl. Phys. **A698** (2001) 253.
6. R. Rapp and J. Wambach, Adv. Nucl. Phys. **25** (2000) 1.
7. G.Q. Li and C. Gale, Phys. Rev. Lett. **81** (1998) 1572.
8. M. Harada and K. Yamawaki, Phys. Rev. Lett. **86** (2001) 757.
9. ALEPH Collaboration (R. Barate *et al.*), Eur. Phys. J. **C4** (1998) 409.
10. E. Braaten, R.D. Pisarski and T.C. Yuan, Phys. Rev. Lett. **64** (1990) 2242.
11. C.H. Lee, J. Wirstam, I. Zahed and T.H. Hansson, Phys. Lett. **B448** (1999) 168.
12. M. Dey, V.L. Eletsky and B.L. Ioffe, Phys. Lett. **B252** (1990) 620.
13. T. Altherr and P. Aurenche, Z. Phys. **C45** (1989) 99.
14. P. Huovinen, M. Belkacem, P.J. Ellis and J.I. Kapusta, e-Print Archive nucl-th/0203023.
15. R. Rapp, Phys. Rev. **C63** (2001) 054907.
16. PHENIX Collaboration (K. Adcox *et al.*), e-Print Arhive nucl-ex/0112006; I. Tserruya, Proc. of ICPAQGP (Jaipur, 26.-30.12.01), to appear in PRAMANA.
17. R. Rapp, Nucl. Phys. **A661** (1999) 33.
18. C.M. Hung and E.V. Shuryak, Phys. Rev. **C56** (1997) 453.
19. P. Huovinen, P.V. Ruuskanen and J. Sollfrank, Nucl. Phys. **A650** (1999) 227.
20. R. Rapp and J. Wambach, Eur. Phys. J. **A6** (1999) 415.
21. G.E. Brown and M. Rho, e-Print Archive hep-ph/0103102; Phys. Rep., to appear.
22. M. Urban, M. Buballa and J. Wambach, Phys. Rev. Lett. **88** (2002) 042002.
23. R. Rapp and E.V. Shuryak, Phys. Lett. **B473** (2000) 13.
24. STAR Collaboration (C. Adler *et al.*), Phys. Rev. Lett. **87** (2001) 082301.
25. R. Auerbeck, private communication.
26. S. Gavin, P.L. McGaughey, P.V. Ruuskanen and R. Vogt, Phys. Rev. **C54** (1996) 2606.
27. PHENIX Collaboration (K. Adcox *et al.*), e-Print Archive nucl-ex/0202002.